Magnetic Resonance in Medicine 49:1098–1105 (2003)

Increased Diffusion Sensitivity With Hyperechos

Lawrence R. Frank,[1,2*] Eric C. Wong,[1] Thomas T. Liu,[1] and Richard B. Buxton[1]

It is shown that the introduction of a 180° refocusing pulse into a standard diffusion weighted stimulated echo sequence is equivalent to the simplest hyperecho sequence with identical diffusion weighting but equal or greater signal-to-noise (SNR) and thus equal or greater diffusion contrast. For high *b*-value imaging, the hyperecho sequence thus possesses the high diffusion contrast in the presence of small T_1/T_2 ratios characteristic of stimulated echo sequences but with less than the 50% loss in SNR that is associated with the stimulated echo. For low *b*-value imaging, the hyperecho signal converges to that of the standard spin echo. The advantages of the two-pulse diffusion weighted hyperecho sequence are demonstrated theoretically. Experimental results are shown in the application to high angular resolution diffusion encoding (HARD) in normal human brain. Magn Reson Med 49: 1098–1105, 2003. Published 2003 Wiley-Liss, Inc.†

Key words: diffusion; hyperechoes; high angular resolution diffusion; diffusion anisotropy

The sensitivity of nuclear magnetic resonance (NMR) to diffusion processes is exquisite and was the focus of some of the earliest experimental studies (1–5). The spin echo method was devised by Hahn in order to overcome field inhomogeneities in the study of diffusion (2). The recognition that relaxation processes impede the acquisition of diffusion-sensitive data motivated the use of stimulated echo methods (6,7), the utility of which derives from the fact that spins continue to accrue diffusion weighting during the "mixing" period between the second and the third 90° pulses but are not subject to transverse relaxation during this period, thereby allowing large diffusion weighting for species with small T_2/T_1 ratios. The cost is that the signal of the stimulated echo is reduced by 50% relative to the spin echo, apart from relaxation effects (4). This underscores the fact that the sensitivity of NMR measurements to diffusion is always problematic, because measurement of diffusion is mediated through signal loss induced by diffusion encoding gradients, which reduces the SNR, and extended diffusion encoding intervals, which further reduces SNR through relaxation related signal loss. For a given *b*-value, the diffusion sensitivity is optimal when the signal is maximum (8) for a given set of relaxation rates T_1, T_2 and local diffusion $\boldsymbol{D}$ of the tissue in question. The influence of these parameters in a pulse sequence depends not only on the pulse sequence timing parameters, but on the coherence pathways that contribute to the final signal (9).

Recently, Hennig (10) introduced the concept of the hyperecho, in which a sequence of refocusing RF excitation pulses of arbitrary flip angle, phase, and intermediate gradient pulses following an initial 90° pulses will refocus to a full echo (in the absence of relaxation or diffusion) following a 180° inversion pulse if they are applied with conjugate symmetry, i.e., negating the order, phase, and flip angle (but the same intermediate gradient pulses). This can be understood as retracing the coherence echo pathways (9) in the time following the 180° pulse until they are once again convergent. The relaxation and diffusion sensitivity of hyperecho sequences is as complex as the details of the different coherence pathways traversed in the formation of the final echo. While the concept of a hyperecho is quite general, applying to an arbitrary number of pulses, we will focus in this article on the simplest case of a two pulse hyperecho (defined as a $\{90_x, \alpha_\phi, 180_y, -\alpha_{-\phi}\}$ sequence) because it can be directly compared with standard spin and stimulated echo acquisitions and because it has the most obvious practical implementation. For this case we prove the remarkable conclusion that the hyperecho sequence theoretically always has optimal diffusion sensitivity compared to standard spin and stimulated echo sequences. The first experimental results of the application of hyperecho diffusion-weighted sequence to a high angular resolution diffusion-weighted scan are shown in a normal human volunteer and compared with an equivalent stimulated echo acquisition. The practical implementation of hyperecho diffusion-weighted imaging presents certain challenges, which are discussed. A preliminary account of this work was recently presented (11).

THEORY

A general hyperecho sequence consists of a set of an initial excitation pulse $90°_x$, then n RF pulses of arbitrary flip angle α_i and phase ϕ_i, $i = 1, \ldots, n$ prior to a $180°_y$ refocusing pulse, which is followed by n conjugate pulses (i.e., flip angle $-\alpha_i$ and phase $-\phi_i$, $i = n, \ldots, 1$) (10). The final amplitude of the hyperecho, including the effects of flip angle, relaxation, and diffusion, is determined by following the individual coherence pathways generated by each pulse and summing the resulting amplitudes at the time of the echo (9). The effect of each RF pulse is to split each magnetization component into a transverse component rotating in phase with the pulse, a transverse component rotating counter phase with the pulse, and a longitudinal component (12,13). Each of these then create a new coherence "pathway" (a trajectory in phase-space) whose amplitude is related to the flip angle. Relaxation and diffusion effects accrue in the intervals between pulses (which are assumed herein to be infinitely short in dura-

[1]UCSD Center for Functional MR1, San Diego, California.

[2]San Diego VA Healthcare System, San Diego, California.

Grant sponsor: VA Merit Review Award (to L.R.F.); Grant number: RO1 NS41925 (to E.C.W.); Grant sponsor: Whitaker and Dana Foundation (to T.T.L.); Grant sponsor: NIH; Grant numbers: 5 R01 NS36722-05; 1 R01 NS42069-01A1 (to R.B.B.).

*Correspondence to: Lawrence R. Frank, Ph.D., UCSD Center for Functional MRI, 9500 Gilman Drive, Mail Code 0677, La Jolla, CA 92093-0677. E-mail: lfrank@ucsd.edu.

Received 1 November 2002; revised 17 January 2003; accepted 20 January 2003.

DOI 10.1002/mrm.10457
Published online in Wiley InterScience (www.interscience.wiley.com).

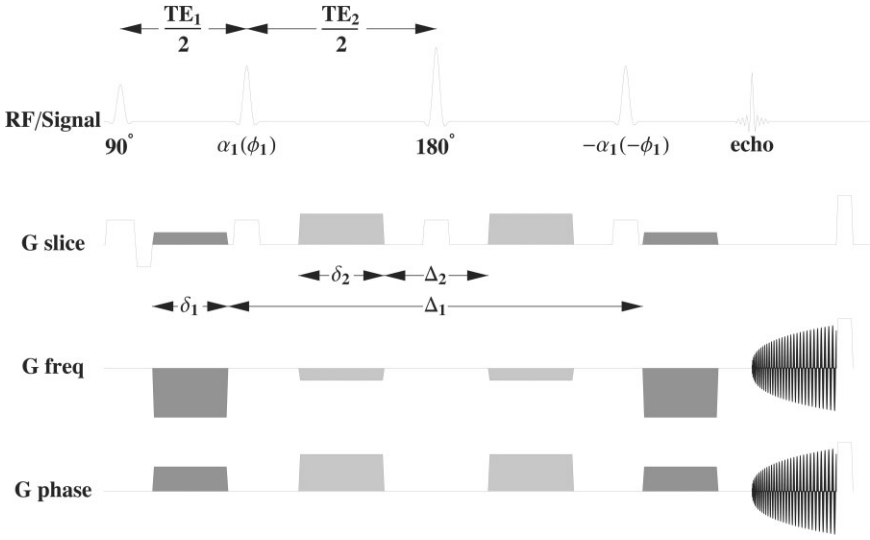

FIG. 1. General two-pulse hyperecho pulse sequence with hyper-diffusion weighting and a spiral acquisition. Note that Δ is defined as the time *between* the diffusion encoding gradients (e.g., Ref. 13), rather than the standard definition.

tion) and scale the echo amplitudes. The final intensity from an echo pathway is the product of the scaling factors due to the RF splitting of the components and the amplitudes factors due to relaxation and diffusion.

For the general case of an arbitrary number of RF pulses, the relaxation and diffusion-weighting depend on all the coherence pathways contributing to the echo and can therefore be quite complicated. It is instructive to consider the simplest hyperecho pulse sequence of two pulses $\{\alpha(\phi), -\alpha(-\phi)\}$ surrounding the 180° refocusing pulse, as shown in Fig. 1. This case is illuminating because for $\alpha = 90°$ this is just a stimulated echo sequence with a 180° refocusing pulse inserted into the middle of the mixing period. This special case we shall refer to as a *hyperstimulated echo* sequence. However, with $\alpha = 0$ this sequence is simply a spin echo experiment. Thus, this sequence lends itself to direct comparison with both the stimulated and spin echo methods.

We consider two cases of diffusion weighting. The first is diffusion-weighting gradients placed only outside the mixing period which we will refer to as "standard" diffusion weighting. In this case the diffusion weighting is identical to both the spin and stimulated echo sequences, thereby allowing direct quantitative comparison of the diffusion sensitivity of the hyperecho, stimulated, and spin echo methods. In the second case, diffusion gradients are placed both inside and outside the mixing period will be referred to as "hyper" diffusion weighting. The coherence pathways for a general hyperstimulated pulse sequence with standard diffusion weighting is shown in Fig. 2. (Note that maintenance of the hyperecho condition requires equal matching gradient areas.) It is assumed that no longitudinal magnetization is generated by T_1 relaxation and hence no new coherence pathways originate at pulses subsequent to the initial excitation.

A general two-pulse hyperecho sequence and the associated timing definitions are shown in Fig. 1. The time $TE_1/2$ is defined as the interval between the 90° excitation pulse and the first hyperecho pulse α_1. The time $TE_2/2$ is defined as the interval between the first hyperecho pulse α_1 and the 180° refocusing pulse. The width of diffusion-weighting gradients is called δ, following standard convention, but the time Δ is defined as the time *between* diffusion gradients, following the definition of Sodickson (13), rather than the standard definition (4). The width of the standard diffusion-weighting gradients is δ_1 and they are placed Δ_1 apart. The diffusion encoding gradient width and separation for the hyper-diffusion weighting are δ_2 and Δ_2, respectively.

The echo intensities of the components generated by the separate coherence pathways are:

$$\text{Stimulated echo:} \qquad I_{ste} = \frac{1}{2} I_0 A \sin^2\alpha \qquad [1a]$$

$$\text{Indirect spin echo:} \qquad I_{ise} = I_0 B \cos^4(\alpha/2) \qquad [1b]$$

$$\text{Direct spin echo:} \qquad I_{dse} = I_0 C \sin^4(\alpha/2) \qquad [1c]$$

where A, B, and C are amplitude factors defined below. The amplitude of the resulting hyperecho is the sum of all the pathways contributing to the echo:

$$\text{Hyper echo:} \qquad I_{he} = I_{ste} + I_{ise} + I_{dse}. \qquad [2]$$

The amplitude factors in Eq. [1] are the products of the independent amplitude coefficients during the interpulse intervals:

$$A = \prod_j^4 A_j, \qquad B = \prod_j^4 B_j, \qquad C = \prod_j^4 C_j. \qquad [3]$$

Each of the individual amplitudes are of the form $A_{i(j)} = E_{i(j)}F_{i(j)}$, where $i = 1, 2$ (similarly for B and C) and where E incorporates T_1 and T_2 relaxation:

$$E_1(\tau) = \exp(-\tau/T_1), \quad E_2(\tau) = \exp(-\tau/T_2) \qquad [4]$$

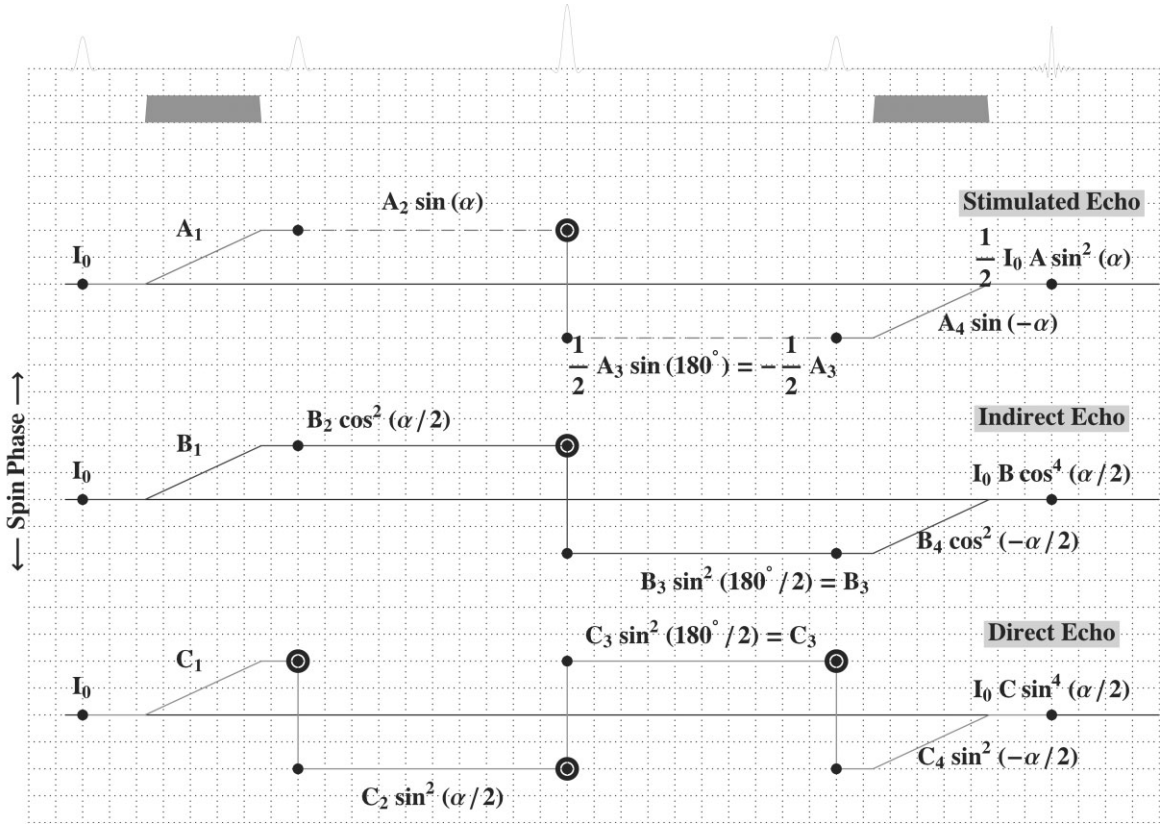

FIG. 2. Coherence pathway diagram (9) for general two-pulse hyperecho sequence with standard diffusion weighting. The vertical axis is the spin phase and the horizontal axis is time. Double circles represent inverted magnetization. A *coherence pathway* is just the phase history of a particular spin population. The convention here is slightly different than in Ref. 9 as no background gradient is assumed, so that only the influence of the diffusion encoding gradients is shown. The amplitudes *A*, *B*, and *C* are given by Eq. [3].

and $F(\tau)$ incorporates diffusion attenuation during a period τ. We will consider here only the standard diffusion weighting because we are interested in the comparison with standard diffusion-weighted sequences. However, the inclusion of hyper-diffusion weighting in the following calculations is straightforward. Here we simplify the notation by writing the diffusion attenuation in terms of a diffusion coefficient D (rather than a diffusion tensor). For notational simplicity we also define $\tau_1 \equiv TE_1/2$ and $\tau_2 \equiv TE_2/2$. From the coherence diagrams in Fig. 2, the echo amplitudes of the individual coherence pathways are shown in Table 1.

Denoting the standard diffusion-encoding gradient G and the hyper-diffusion-encoding gradient g, the diffusion attenuations are:

$$F_G(\delta_1) = \exp(-Dk_{\max}^2\delta_1/3) \qquad [5a]$$

Table 1
Amplitudes of Separate Echo Pathways

Stimulated echo	Indirect echo	Direct echo
$A_1 = E_2(\tau_1)F_G(\delta_1)$	$B_1 = E_2(\tau_1)F_G(\delta_1)$	$C_1 = E_2(\tau_1)F_G(\delta_1)$
$A_2 = E_1(\tau_2)F_g(\Delta_1/2)$	$B_2 = E_2(\tau_2)F_g(\Delta_1/2)$	$C_2 = E_2(\tau_2)F_g(\Delta_1/2)$
$A_3 = E_1(\tau_2)F_g(\Delta_1/2)$	$B_3 = E_2(\tau_2)F_g(\Delta_1/2)$	$C_3 = E_2(\tau_2)F_g(\Delta_1/2)$
$A_4 = E_2(\tau_1)F_G(\delta_1)$	$B_4 = E_2(\tau_1)F_G(\delta_1)$	$C_4 = E_2(\tau_1)F_G(\delta_1)$

$$F_g(\Delta_1/2) = \exp(-Dk_{\max}^2\Delta_1/2) \qquad [5b]$$

where $k_{\max}$ is the maximum k-space excursion reached before the application of the RF pulse. $F_G(\delta_1)$ is the diffusion attenuation during the standard diffusion-encoding period. In the present case of a linear gradient, $k_{\max} = \gamma G\delta_1$ during the diffusion-encoding gradients. $F_g(\Delta_1/2)$ is the diffusion attenuation during the mixing period Δ_1. We have considered here only the case of standard diffusion weighting, as expressed by $F_g(\Delta_1/2)$ where $g = 0$. Hyper-diffusion weighting, where diffusion gradients are added inside the mixing period, is more complicated as these gradients affect only the spin echo pathways and not the stimulated echo pathway. This is further complicated by the interaction between the diffusion-encoding gradients inside and outside the mixing period. Our implementation of the hyperecho pulse sequence is designed to eliminate all coherence pathways other than those depicted in Fig. 2. Generally, however, in a sequence containing 4 RF pulses, there are multiple coherence pathways, including those generated as a result of relaxation, which may have different diffusion weightings in the presence of hyper-diffusion gradients, making quantification of diffusion sensitivity more difficult.

The amplitude factors *A*, *B*, and *C* that scale the intensities of the individual echo pathways in Eq. [1] can be

determined by substituting the amplitudes defined in Table 1 into Eq. [3]:

$$A = E_2^2(\tau_1)E_1^2(\tau_2)F_G^2(\delta_1)F_g^2(\Delta_1/2) \quad [6a]$$

$$B = C = E_2^2(\tau_1)E_2^2(\tau_2)F_G^2(\delta_1)F_g^2(\Delta_1/2). \quad [6b]$$

For the case $g = 0$, which represents standard diffusion weighting (i.e., no diffusion weighting in the mixing period), these amplitudes are:

$$A = e^{-(2\delta_1/T_2+\Delta_1/T_1)}e^{-D\gamma^2G^2\delta_1^2(\Delta_1+2\delta_1/3)} \quad [7a]$$

$$B = C = e^{-(2\delta_1+\Delta_1)/T_2}e^{-D\gamma^2G^2\delta_1^2(\Delta_1+2\delta_1/3)}. \quad [7b]$$

The diffusion attenuation for the spin echo and stimulated echo pathways are all equivalent, since the diffusion weighting is proportional to k^2 so that inversion has no influence on the attenuation. Note that the time factor $(\Delta_1 + 2\delta_1/3)$ in Eq. [7] with Δ_1 defined as the time *between* the diffusion-weighting gradients (13) is equivalent to the more recognizable factor $(\Delta_1 - \delta_1/3)$ produced by the more standard definition of Δ_1 as the time between the *start* of the diffusion encoding gradient (4).

Using the fact that, from Eq. [7], the amplitudes B and C from the spin echo pathways are equal, Eq. [1] allows the hyperecho intensity (Eq. [2]) to be written in terms of the separate contributions from the stimulated and spin echo pathways:

$$\frac{I_{he}}{I_0} = \underbrace{\frac{1}{2}A\sin^2\alpha}_{\text{Stimulated echo}} + \underbrace{\frac{1}{4}B[3+\cos(2\alpha)]}_{\text{Spin echo}}. \quad [8]$$

A useful way to rewrite Eq. [8] is in the form:

$$\frac{I_{he}}{I_0} = \frac{1}{4}A\{2\sin^2\alpha + f[3+\cos(2\alpha)]\} \quad [9]$$

where, using the amplitudes in Eq. [7], the ratio of the spin echo to stimulated echo amplitudes is given by:

$$f \equiv \frac{B}{A} = e^{-\Delta_1(R_2-R_1)} \quad [10]$$

where the $R_i = 1/T_i$ are the relaxation rates. The factor f accounts for the signal loss due to the relative contributions of T_1 and T_2 relaxation from both the spin and stimulated pathways. In the absence of relaxation ($R_1 = R_2 = 0$), $f = 1$ in which case $A = B$ and the ratio depends only on the diffusion-related signal loss of a standard diffusion-weighted spin echo sequence, independent of the flip angle α, since $\frac{1}{4}\{2\sin^2\alpha + [3 + \cos(2\alpha)]\} = 1$. If there is also no diffusion, $(B(R_1 = R_2 = D = 0) = 1)$, and the ratio of the hyperecho signal to the initial intensity is $I_{he}/I_0 = 1$, and thus the hyperecho recovers all of the magnetization, independent of α, as predicted (10).

For the case with relaxation where $f \neq 1$, the ratio I_{he}/I_0 now depends on the flip angle α. For a given set of relaxation and diffusion parameters, the optimal hyperecho signal is found by maximizing Eq. [9] with respect to variations in α, which provides the optimal flip angle α_{opt}:

$$\frac{\partial}{\partial\alpha}\{2\sin^2\alpha + f[3+\cos(2\alpha)]\} = 0 \Rightarrow |\alpha_{opt}| = \frac{\pi}{2} \quad [11]$$

which is precisely the special case of the hyperstimulated echo sequence. The result in Eq. [11] is intuitively clear because a 90° pulse maximizes the stimulated echo signal contribution and thus the total signal in the presence of relaxation. Substituting Eq. [11] into Eq. [9] yields:

$$\frac{I_{he}}{I_0} = \frac{1}{2}A(1+f). \quad [12]$$

In the limit of a large $\xi = \Delta_1(R_2 - R_1)$, either because of a large difference between relaxation rates or a long mixing time, $\lim_{\xi\to 0} f = 0$ and the ratio $I_{he}/I_0 \to A/2$, the stimulated echo intensity. In the limit $\lim_{\Delta_1\to 0}$, which approaches the case of a spin echo, $I_{he}/I_0 \to 1$ and the full signal is recovered. In the limit of a small $\xi = \Delta_1(R_2 - R_1)$, either because of similar relaxation rates or a short mixing time, $\lim_{\xi\to 0} f = 1 \Rightarrow A \approx B$ and the ratio $I_{he}/I_0 \to 1$, reflecting a recovery of the complete coherence pathways, the signature of the hyperecho (10).

The important point is that, because the hyperecho refocuses all of the available magnetization, its diffusion sensitivity will *always* be greater than that of its component pathways, because the fractional diffusion-related signal loss is the same and the signal, from Eq. [2], is composed of the sum of the spin and the stimulated echo pathways. The special case of the hyperstimulated echo sequence discussed in detail here was chosen to demonstrate this because it is the simplest hyperecho sequence and direct comparisons can be made with standard spin and stimulated echo sequences, which compose its relevant component pathways. Moreover, from Eq. [11], it has the largest hyperecho signal in the presence of relaxation and diffusion. With standard diffusion weighting (i.e., diffusion-weighted gradients only outside the mixing period) the diffusion weighting of all three methods are identical, allowing direct comparison of the diffusion sensitivities. Of particular interest is the comparison with the stimulated echo for large b-value imaging in the presence of small T_2/T_1 ratios characteristic of biological tissues.

SIMULATIONS

The theoretical predictions can be demonstrated by simulating the signals as a function of b-value for realistic tissue parameters. Diffusion-weighted imaging involves a tradeoff between the production of diffusion-related signal loss to measure diffusion through both large diffusion-weighting gradients and long diffusion-encoding times and the concomitant reduction in SNR from diffusion-induced signal loss and relaxation-related signal loss, respectively, that degrade such measurements. Judging the relative diffusion sensitivities of different sequences can be done by determining which has the largest diffusion contrast C, defined as the difference of the signal with and

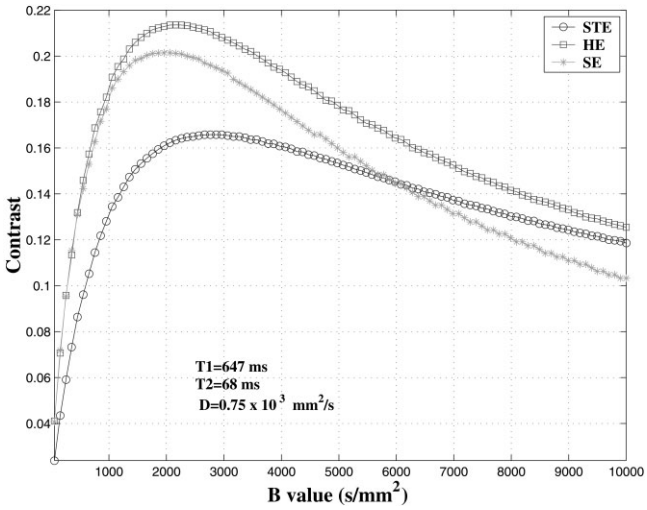

FIG. 3. Simulated diffusion contrast curves for spin echo (SE), stimulated echo (STE), and hyperstimulated echo (HE) pulse sequence for white matter. For small *b*-values, the HE and SE contrasts converge. For high *b*-values, the HE and STE contrasts converge. In the intermediate region, however, the HE contrast has significant contributions from both the SE and STE pathways and so has greater contrast than either pathway individually.

without diffusion weighting (8). The "optimal" sequence will be the one that produces the highest signal for the given *b*-value. Because the signal from both stimulated and hyperecho are functions of the two timing parameters Δ_1 and δ_1, however, determination of this optimal value involves a search over the 2D parameter space $C(\Delta_1, \delta_1)$.

An example for the special case of the hyperstimulated echo with standard diffusion weighting is shown in Fig. 3 for white matter at 1.5 T (T_1 = 647 ms, T_2 = 68 ms, D = 0.75 $\times 10^{-3}$ mm^2/s, (14,15). Points on these curves are generated for each *b*-value by searching through the parameter space (δ_1, Δ_1), for a fixed gradient strength (set to the maximum g = 2.2 G/cm of our system), to find the pairs that result in this *b*-value, of which there may be many. For all such pairs that produce a given *b*-value, the one that produces the highest contrast is chosen and plotted. There are several points of interest in Fig. 3. At low *b*-values, the hyperecho signal is dominated by the spin echo pathway and therefore shows the expected SNR gain of 2 over the stimulated echo. For large *b*-values, the hyperecho and stimulated echo intensities converge as the influence of the spin echo pathways dies aways via T_2 relaxation. At the other extreme near low *b*-values, the hyperecho and spin echo intensities converge, as the signal loss from diffusion and relaxation is reduced. However, throughout a wide range of *b*-values the hyperecho signal produces greater diffusion contrast than the separate spin or stimulated echo pathways, because each of these pathways contributes significantly to the overall echo intensity. Thus, the long-held belief that one must sacrifice 50% of the signal to get diffusion weighting in tissues with large T_1/T_2 ratios by using a stimulated echo is not the case for all realistic combinations of parameters.

The implications for diffusion-weighted imaging are profound, as throughout the entire range of *b*-values the hyperstimulated echo contrast is greater than or equal to that of both the spin and the stimulated echo. However, there are significant technical difficulties in guaranteeing the hyperecho condition in the presence of large diffusion gradients, as discussed in the next section.

METHODS

Basic Spiral Acquisition

Images were acquired on a GE SIGNA 1.5 T Clinical Imager with high-speed gradient hardware using a spiral acquisition. Diffusion sensitive images were acquired on normal human subjects, with approval from the Humans Subject Committee at UC San Diego, using the hyperecho sequence depicted in Fig. 4, which employs a spiral readout. The spiral acquisition is that designed by Glover (16), based on the work of Meyer et al. (17), optimized to acquire data at a maximum rate within the limits of gradient amplitude and slew rate achievable by our scanner. Fat suppression was always employed. Our protocols always use the minimum echo time consistent with the chosen diffusion weighting. The pulse sequence was designed to operate in spin, stimulated, and hyperecho modes. This enabled keeping all imaging and diffusion-weighting parameters the same except for those defining the excitation modes. For all the hyperecho results shown herein standard diffusion weighting, that is, only external to the mixing time Δ_1 was employed.

HARD Encoding

High angular resolution diffusion encoding (HARD) was achieved by generating gradient directions equally spaced on a sphere by tessellations of an icosahedron, as previously described (18,19). Single shot images were acquired at three slices with the following parameters: FOV = 24 cm, slice thickness = 3.8 mm, and matrix size 64 $\times$ 64 for approximately (3.75 mm $\times$ 3.75 mm $\times$ 3.8 mm) isotropic resolution, TR = 2700 ms, TE = 52 ms. The diffusion parameters were: diffusion gradient duration, δ_1 = 48 ms, mixing time Δ_1 = 173 ms, and $b \approx$ 2848 s/mm^2, and 42 diffusion directions. The values of Δ_1 and δ_1 where chosen at the peak of the hyperecho diffusion contrast curve in Fig. 3. Twenty averages at each diffusion direction were collected to ensure high SNRs and resulted in a total scan time of $\approx$34 min.

Eddy Current Compensation

The hyperecho condition is extremely sensitive to phase errors because it requires complete phase coherence across multiple pathways. Eddy currents are therefore one significant source of error since they produce spatially varying phases that result in spatially varying magnitudes in hyperecho images. In the protocol utilized here, the diffusion-encoding gradients are the primary culprit in the generation of eddy currents. Because gradient-induced eddy currents are dependent on the scanner geometry, they are gradient direction-dependent, with the unfortunate consequence that high angular resolution diffusion-weighted (HARD) measurements induce different eddy currents with every diffusion encoding direction. The re-

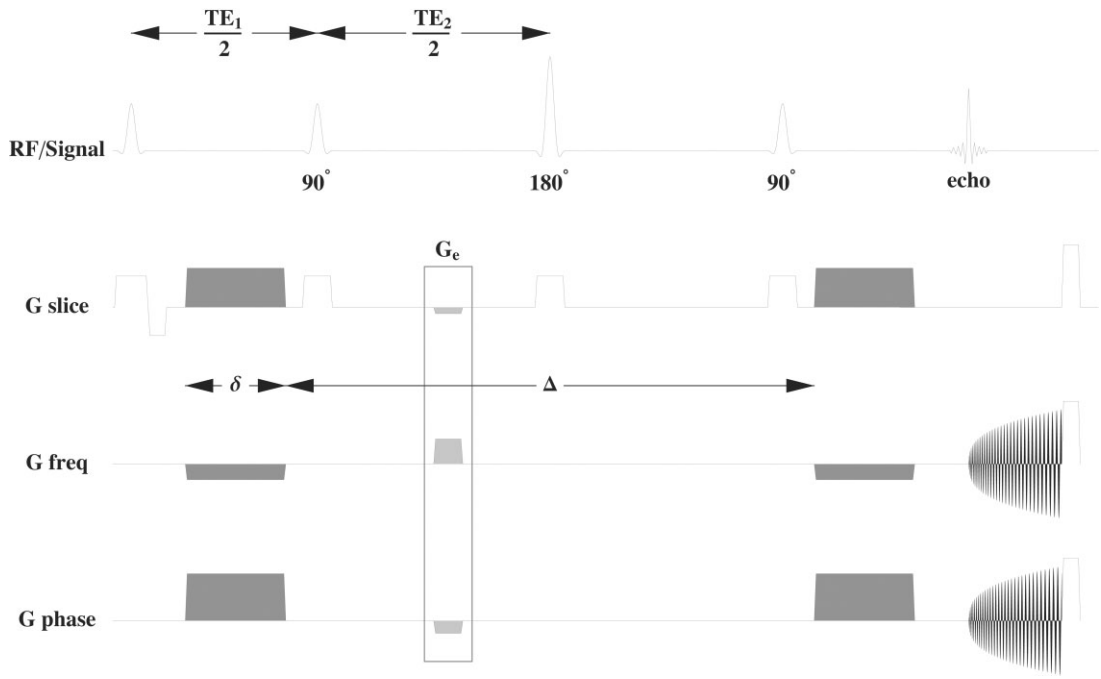

FIG. 4. Diffusion-weighted hyperstimulated echo pulse sequence with eddy current compensation achieved by a small corrective gradient lobe (G_e) along the diffusion-weighting directions. Diffusion weighting was applied only outside the mixing time Δ to make it equivalent to the corresponding stimulated echo sequence.

sult is a strong spatial variation in hyperecho intensity and a concomitant variation in anisotropy unrelated to diffusion. An example is shown in Fig. 5a.

However, the phase errors produced in the sequence were approximately linear in the direction of the diffusion gradient. This is apparent in Fig. 5a as an approximately linear shading across the images of anisotropy. This dominant linear term can be compensated for by the application of a small gradient pulse which is rotated in concert with the diffusion-encoding directions. In this view, the eddy currents can be seen as producing a net gradient area that partially destroys the hyperecho condition, for which the compensating gradient corrects. Such a compensating pulse was added to the pulse sequence used in this study, as shown in Fig. 4. Using this method produced images with eddy current artifacts greatly reduced, as shown in Fig. 5b. In the present work, the eddy current compensation pulse was tuned manually. However, since eddy current compensation is a critical factor in the integrity of the hyperecho diffusion-weighted images and yet varies with the HARD encoding parameters, manual tuning is impractical as a general method. An automated scheme for adjusting the correction gradient lobe is currently under development in our laboratory.

RESULTS

In Fig. 6b are shown the results from the HARD encoding hyperecho sequence using standard diffusion weighting. The equivalent stimulated echo images shown in Fig. 6a. The data shown are the energy in the single fiber (i.e., $L = 2$) channel of the spherical harmonic decomposition

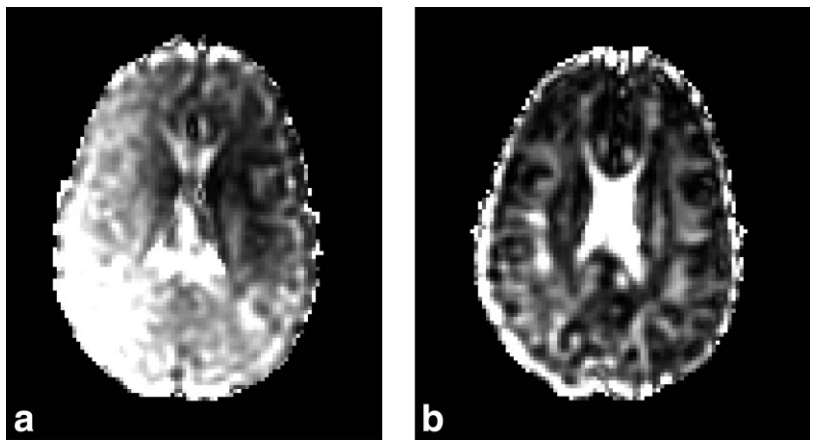

FIG. 5. Spherical diffusion variance maps (19) from diffusion-weighted hyperechos (**a**) without and (**b**) with eddy current compensation. The approximately linear (in space) shading of the amplitude in **a** is caused by the approximately linear eddy current induced spatial phase variations. The eddy current compensation scheme shown in Fig. 4 corrects for this dominant linear error and significantly reduces the eddy current effects, as seen in **b**. Residual errors, however, are still evident in the spuriously bright border between the brain and the background.

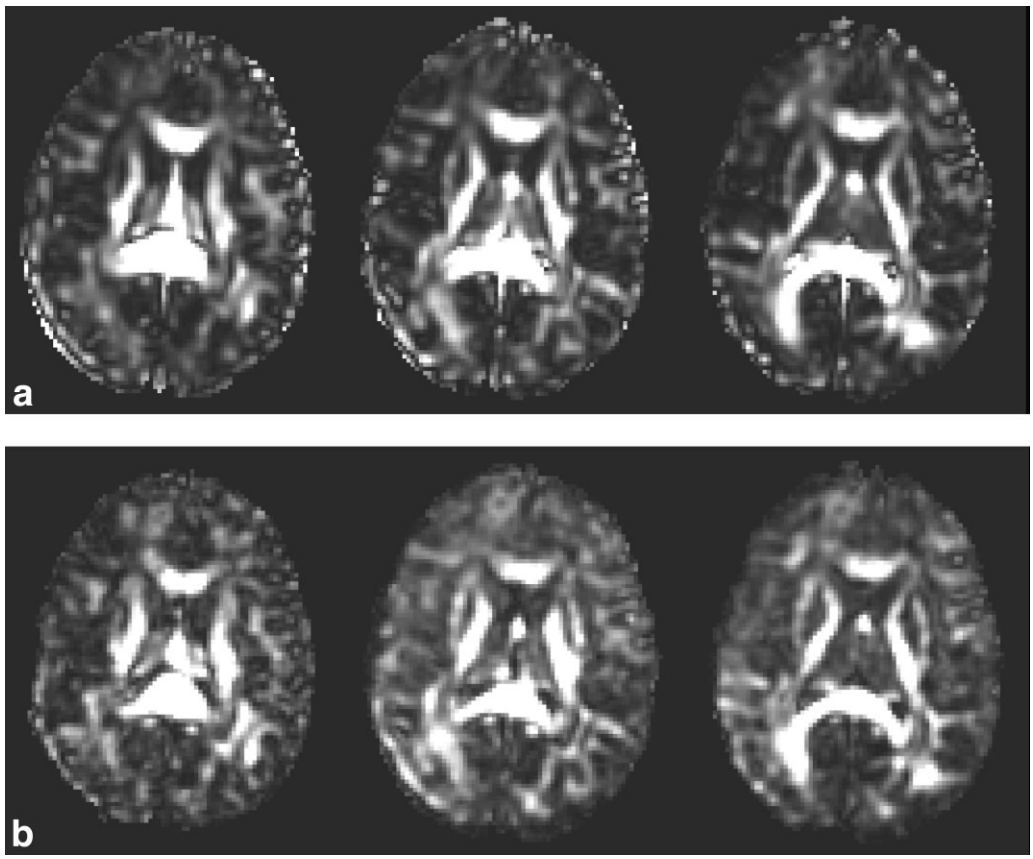

FIG. 6. Anisotropy maps derived from HARD encoded (**a**) stimulated echo and (**b**) hyperecho images acquired with identical diffusion weighting. The pulse sequenced used to acquire these images were identical in all parameters (see text) except for the addition of the 180° pulse in **b** to form the hyperecho, in addition to the small eddy current compensating gradients. Maps shown are the energy in the single fiber channel of the spherical harmonic decomposition (20), equivalent to the information in a diffusion tensor anisotropy map.

(SHD) of the data (20). This is equivalent to the information in a standard DTI anisotropy map, with one significant difference that is critical for the present application. The SHD decomposes the apparent diffusion coefficient into spherical harmonic components of all orders L up to $L_{\max}$: $L = 0, 1, \ldots, L_{\max}$. However, by symmetry, only the even orders describe diffusion, whereas the odd channels contain energy related to experimental artifacts (20). Since eddy current effects have a significant amount of their energy in the $L = 1$ channel which characterizes linear offsets, the SHD can significantly reduce their effects. These effects are not eliminated, however, as eddy currents also produce energy in the other (even) channels.

The results shown in Fig. 6a,b are nearly identical in appearance and attest to the ability to acquire HARD encoded hyperecho images. A quantitative assessment of the theoretical advantages outlined in the theory, however, will require a significant reduction in the eddy current effects. This is currently under way in our laboratory. However, a homogeneous phantom imaged on the same scanner with the same hyperstimulated echo pulse sequence produced images with approximately 28% higher mean intensity over a region of interest than that of the corresponding stimulated echo image, while possessing the same diffusion weighting. In principle, given the results in Fig. 3, a more fair comparison of the hyperecho data in Fig. 6a would be with a spin echo image of the same diffusion weighting. However, such a sequence would necessarily have a larger echo time and longer gradients, resulting in significantly different eddy current effects. The stimulated echo and hyperstimulated echo, on the other hand, differ only in the addition of a 180° pulse to the latter, with all other parameters being identical. It is thus more amenable to direct experimental comparison. Methods for eddy current artifact reduction and subsequent quantitative investigation of hyperecho pulse sequence optimization is currently under way in our laboratory.

DISCUSSION AND CONCLUSION

A common theme in the history of diffusion NMR and MRI is the necessary tradeoff between diffusion sensitization, which occurs through diffusion-encoding gradients that produce signal loss and the resulting loss in SNR that degrades the data. This occurs both because of the diffusion-related signal loss designed to be measured and relaxation effects which grow with the extension of the diffusion-encoding intervals.

The issue of diffusion sensitivity vs. SNR has become a central concern of late with the understanding that many tissues, such as white matter, possess complex geometries

through which diffusion can trace complex paths. This, combined with the inherent spatial limitations of MR imaging, produce voxels in which the diffusion can be highly complex. The original diffusion tensor imaging (DTI) formulation of Basser et al. (21) showed that if the diffusion was contained in a single bundle of straight fibers within a voxel, then with a small number of measurements (6) sampled at equal angles on the surface of a sphere, it is possible to completely characterize the diffusion as a tensor that describes the diffusion along three orthogonal directions in a coordinate system oriented at some angle relative to the scanner coordinate system. This method is not strongly dependent on the magnitude of the diffusion sensitization (characterized by the *b*-factor).

When this "single fiber approximation" (i.e., DTI) breaks down, however, the problem becomes significantly more complicated. This problem was elucidated by Tuch et al. (18), who recognized that two additional factors must be introduced in order to measure diffusion under such circumstances. The first is finer angular sampling, which is called high angular resolution diffusion weighting (HARD). The second is the necessity of high *b*-values for distinction between diffusion compartments, a problem not unique to HARD imaging but existent even in the simplest case of a two-component diffusion in a liquid (19). Taken together, these two additions admit a generalization of the concept of DTI to higher-order tensors to characterize complex diffusion (20). Attaining this additional information, however, requires longer scan times and lower SNR. It is important to remember that scan time is proportional to $(SNR)^2$, so the increased SNR provided by the diffusion-weighted hyperecho sequence over traditional methods can lead to a significant reduction in scan time for an equivalent SNR.

The necessity for high *b*-values brings the issue of SNR reduction to the forefront. This is particularly true in biological tissues where large differences between T_1 and T_2 suggest the optimality of a stimulated echo diffusion weighted acquisition, along with its inherent factor of 2 loss of signal. In this article we have shown that this historically accepted fact of a loss of a factor of 2 in SNR is, in fact, not a requirement, for the addition of a 180° pulse refocuses the "lost" magnetization while retaining the same diffusion weighting, thus increasing the diffusion sensitivity. While the concept of a hyperecho introduced by Hennig (10) is quite general, applying to an arbitrary number of pulses, we have focused here on the simplest case of a two pulse hyperecho because it can be directly compared with standard spin and stimulated echo acquisitions. In particular, we have shown that the addition of a 180° pulse into a standard stimulated echo acquisition is a special case of the simplest hyperecho sequence, which we have termed a *hyperstimulated echo* sequence (i.e., a two-pulse hyperecho sequence with $\alpha = 90°$), has optimal diffusion sensitivity for the two-pulse hyperecho sequence, and *always* has greater diffusion sensitivity than both the spin and stimulated echo sequence. Although the necessity for phase integrity is critical for retention of the hyperecho condition and poses a challenge for pulse sequence development, our initial results suggest the utility of the incorporation of hyperecho diffusion weighting into existing schemes for high *b*-value diffusion imaging, and the possibility of increased diffusion sensitivity over traditional methods in a wide variety of applications.

REFERENCES

1. Carr HY, Purcell EM. Effects of diffusion on free precession in nuclear magnetic resonance experiments. Phys Rev 1954;94:630–638.
2. Hahn EL. Detection of sea-water motion by nuclear precession. J Geophys Res 1960;65:776.
3. Woessner DE. Effects of diffusion in nuclear magnetic resonance spin-echo experiments. J Chem Phys 1961;34:2057–2061.
4. Stejskal EO, Tanner JE. Spin diffusion measurements: spin echoes in the presence of a time dependent field gradient. J Chem Phys 1965;42:288–292.
5. Stejskal EO. Use of spin echoes in a pulsed magnetic field gradient to study anisotropic, restricted diffusion and flow. J Chem Phys 1965;43:3597–3603.
6. Tanner JE. Use of the stimulated echo in NMR diffusion studies. J Chem Phys 1970;52:2523–2526.
7. Tanner JE. Transient diffusion in system partitioned by permeable barriers. Application to NMR measurements with a pulsed field gradient. J Chem Phys 1978;69:1748–1754.
8. Zauscher B, Frank LR. Optimization of diffusion weighted pulse sequences using a stimulated echo spiral sequence. In: Proc 9th Annual Meeting, ISMRM, Glasgow, 2001.
9. Hennig J. Multiecho imaging sequences with low refocusing flip angles. Magn Reson Med 1988;78:397–407.
10. Hennig J, Scheffler K. Hyperechoes. Magn Reson Med 2001;46:6–12.
11. Frank LR, Wong EC, Liu TT, Buxton RB. Increased diffusion sensitivity with hyperechoes. In: Proc 10th Annual Meeting, ISMRM, Honolulu, 2002. p 434.
12. Scheffler K. A pictorial description of steady states in rapid magnetic resonance imaging. Concepts Magn Reson 1999;11:291–304.
13. Sodickson A, Cory DG. A generalized k-space formalism for treating the spatial aspects of a variety of NMR experiments. Prog Nuclear Magn Reson Spectrosc 1998;33:77–108.
14. Pierpaoli C, Basser PJ. Towards a quantitative assessment of diffusion anisotropy. Magn Reson Med 1996;36:893–906.
15. Pierpaoli C, Jezzard P, Basser PJ, Barnett A, DiChiro G. Diffusion tensor MR imaging of the human brain. Radiology 1996;201:637–648.
16. Glover GH. Simple analytic spiral k-space algorithm. Magn Reson Med 1999;42:412–415.
17. Meyer CH, Hu BS, Nishimura DG, Macovski A. Fast spiral coronary artery imaging. Magn Reson Med 1992;28:202–213.
18. Tuch DS, Weisskoff RM, Belliveau JW, Wedeen VJ. High angular resolution diffusion imaging of the human brain. In: Proc 7th Annual Meeting, ISMRM, Philadelphia, 1999. p 321.
19. Frank LR. Anisotropy in high angular resolution diffusion weighted MRI. Magn Reson Med 2001;45:935–939.
20. Frank LR. Characterization of anisotropy in high angular resolution diffusion weighted MRI. Magn Reson Med 2002;47:1083–1099.
21. Basser PJ, Mattiello J, LeBihan D. Estimation of the effective self-diffusion tensor from the NMR spin echo. J Magn Reson 1994;103:247–254.